Monatshefte für Chemie 135, 1157–1166 (2004)
DOI 10.1007/s00706-004-0186-6

Monatshefte für Chemie
Chemical Monthly
Printed in Austria

Synthesis and Properties of 10,11-Dibenzimidazolyl-10,11-didesmethylhypericin – The First Heterocyclically Substituted Hypericin Derivative[#]

Bernd Lackner, Christoph Etzlstorfer, and **Heinz Falk***

Institute of Organic Chemistry, Johannes Kepler University, A-4040 Linz, Austria

Received January 15, 2004; accepted February 8, 2004
Published online June 24, 2004

Summary. The synthesis of the first heterocyclically substituted title hypericin derivative was achieved starting from 6-benzimidazolyl-tri-*O*-methyl-6-desmethylemodin. The chemical as well as photochemical properties of this unique hypericin derivative, which might constitute a new photodynamic therapy agent, are reported.

Keywords. Heterocycles; Phenanthroperylenequinone; Photodynamic therapy; Semiempirical calculations; Tautomerism.

Introduction

The well known naturally occuring phenanthroperylenquinone hypericin (**1**) is of particular interest because of its outstanding photosensitizing properties, especially for its application in photodynamic tumor therapy [1–4]. Hypericin is also important for its broad anticancer and antiviral activity [5–7]. Over the last decade a broad variety of modified hypericin derivatives have been synthesized in our group for studying the photochemical and photobiological behaviour of these compounds [2–4, 8–14]. Presently, we are strenously pursuing to achieve a bathochromic shift of the long wavelength absorption band of **1**, which is essential for an improved effectiveness of hypericin derivatives as photodynamic therapy drugs.

For this purpose we have developed the synthesis of tri-*O*-methyl protected emodin aldehyde and nitrile [15], which have provided access to a wide variety of modified tri-*O*-methylemodin derivatives. In particular, the class of 6-heterocyclically appended tri-*O*-methyl protected 6-desmethylemodin derivatives [16] synthesized recently are of interest as promising synthons for the synthesis of

* Corresponding author. E-mail: heinz.falk@jku.at

[#] Dedicated to Prof. Dr. *K. Schlögl* on occasion of his 80th birthday

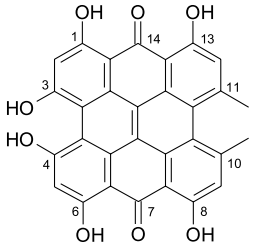

1

heterocyclically appended hypericin derivatives. Herein, we report our efforts to prepare and investigate 10,11-dibenzimidazolyl-10,11-didesmethylhypericin (**5**), which is the first heterocyclically substituted hypericin derivative.

Results and Discussion

Synthesis

Starting from 6-benzimidazolyl-tri-*O*-methyl-6-desmethylemodin (**2**), which displays a significant bathochromic shift of the long wavelength absorption band ($\lambda_{max} \sim 418$ nm) in comparison to its parent compound, tri-*O*-methylemodin ($\lambda_{max} \sim 402$ nm), the synthesis of the dibenzimidazolyl didesmethyl hypericin **5** was performed in three steps (Scheme 1). Thus, reduction/deprotection of **2** to the corresponding anthrone **3** by refluxing a mixture of **2**, $SnCl_2 \cdot 2H_2O$, and HBr in glacial acetic acid [17] for 1 h under Ar provided **3** in 94% yield. Dimerization of **3** was carried out in the conventional way [18] using a stirred solution of **3**, $FeSO_4 \cdot 7H_2O$, pyridine-*N*-oxide, piperidine, and pyridine under Ar and light protection. Heating at 115°C for 1 h yielded a mixture of the protohypericin derivative **4** and the corresponding light induced photocyclisation product **5**. Upon irradiation of this mixture **4** was completely cyclized to the desired hypericin derivative **5**, which was isolated as a dark green solid in 85% overall yield based on **3** (Scheme 1).

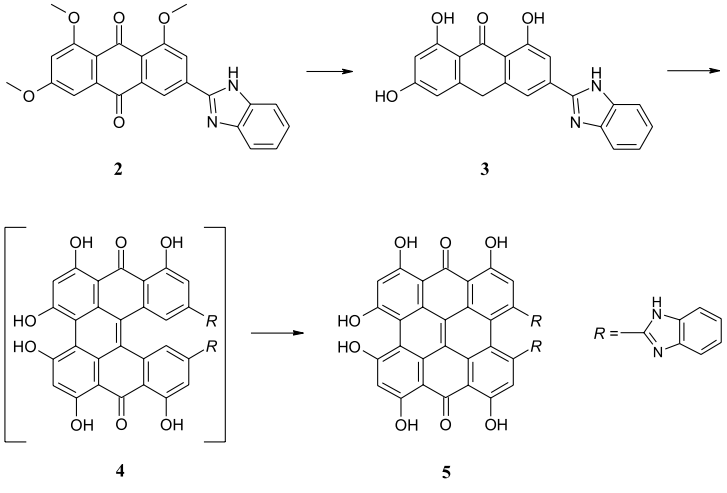

2 **3** **4** **5**

Scheme 1

Chemical and Photochemical Properties

A series of investigations were undertaken to determine the chemical behaviour of the heterocyclically substituted hypericin derivative **5**. Thus, for the application of **5** as a potential drug in photodynamic therapy, it is of particular interest that this new compound fulfils three main properties, namely a bathochromic shift of the long wavelength absorption band, the ability of generating singlet oxygen or reactive oxygen species, and last but not least, a proper solubility under physiological conditions.

Fortunately, a remarkable bathochromic shift of the long wavelength absorption band depending on the solvent is observed. Accordingly, the bathochromic shifts in ethyl acetate, *DMF*, *DMSO*, and pyridine were in the range of $\Delta\lambda_{max} \sim 75$ nm, while in acetone, acetonitrile, methanol, and *THF* the shifts were $\Delta\lambda_{max} \sim 46$ nm in comparison to hypericin (**1**) ($\lambda_{max} \sim 598$ nm). Therefore one of the major targets, the shifting of the long wavelength absorption band of hypericin towards the emission wavelength range of medicinal lasers ($\lambda_{max} > 620$ nm) was achieved by the synthesis of **5**. Regarding the solubility of **5** it is noteworthy that it is poorly soluble in acetone, acetonitrile, ethyl acetate, water, and methanol. However, by means of a small amount of *DMSO* (~5%) added as a solution mediator, **5** shows also a proper solubility (~0.1 mg · cm^{-3}) in these solvents. The molar extinction coefficient of the long wavelength absorption band of **5** in *DMF*, *DMSO*, 80% aqueous *DMSO*, and pyridine is in the range of $\varepsilon = 5\,000$ dm^3 · mol^{-1} · cm^{-1}, which amounts to approximately one thenth of that observed for hypericin (**1**) itself.

The results of the spectrophotometric titration of **5** in 80% aqueous *DMSO* shown in Fig. 1 describe the protonation and deprotonation behaviour of **5**. It became evident that, depending on the *pH* values of the 80% aqueous *DMSO* solutions, a certain species dominated below $pH \sim 1$, another one prevailed at $pH \sim 3$, followed by a third species predominant at $pH \sim 6.5$, and finally a fourth one became prominent above $pH \sim 10.5$. Fluorescence experiments at different *pH* values indicated also the presence of different species depending on the *pH* value, which corroborates the spectrophotometric titration results. Accordingly, the low

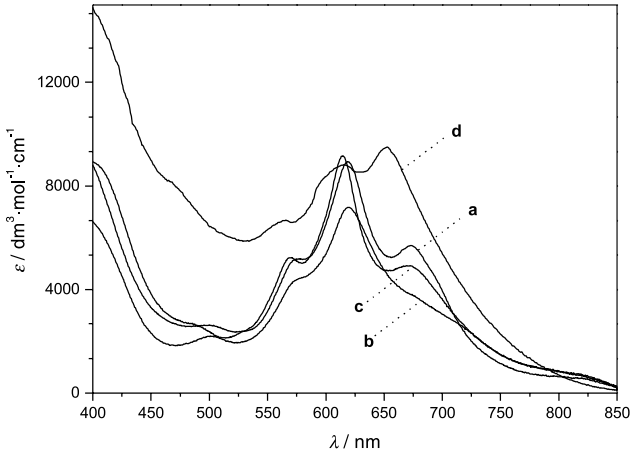

Fig. 1. Absorption spectra of **5** in 80% aqueous *DMSO* at $pH = 1.0$ (a), 3.0 (b), 6.4 (c), and 10.5 (d) (titration with H_2SO_4 or *TBAH*); the ε-values were corrected for adsorbed methanol and water (*cf.* Experimental)

extinction coefficient of **5** might be due to the presence of several differently absorbing species and association phenomena as evident from *Lambert-Beer* dilution experiments on 80% aqueous *DMSO* solutions.

Of course, the modification of **1** by the two benzimidazolyl substituents is responsible for the complexicity of the protonation and deprotonation behaviour of **5**. This is based on the fact, that benzimidazole itself with $pK_a{}^1 \sim 13.2$ and $pK_a{}^2 \sim 5.5$ [19] can act as a proton donor as well as a proton acceptor. Since the *bay*-hydroxyl groups of hypericin (**1**) are strongly acidic ($pK_a \sim 2$ [20]), it is obvious that **5** with its basic benzimidazolyl substituents has the possibility of forming a zwitterion *via* protonation of the benzimidazolyl nitrogen involving the proton of the *bay*-hydroxyl group. It was not possible to find direct evidence for the existence of this zwitterion of **5**, but it could be unequivocally established by means of electrospray mass experiments [21], that the species predominant within the *pH* range of 6.4–12.0 is the monodeprotonated species $\mathbf{5}^{(-)}$ characterized by $m/z = 707$. At *pH* ranges below 6 no signal could be detected. Thus, the ''delayed'' appearance of the $\mathbf{5}^{(-)}$ ion above *pH* 6 in comparison with that of $\mathbf{1}^{(-)}$ might constitute an indirect evidence for the existence of the zwitterion between *pH* 3 and 6. Accordingly, we may assign to the species present below *pH* 3 the monoprotonated form $\mathbf{5} \cdot H^+$, between *pH* 3 and 6 the zwitterion **5**, above *pH* 6 the monodeprotonated form $\mathbf{5}^{(-)}$, and above *pH* 10 the dideprotonated form $\mathbf{5}^{(2-)}$. Beside the possibility of **5** to form an internal salt it is also conceivable that tautomerism within the system of **5** plays a role in the chemical behaviour of this compound.

The structural assignment of **5** was performed *via* its characteristic IR absorption bands, mass spectra, and the results of an elemental analysis, which in particular shows that in addition to the target compound **5**, tight inclusions of water and methanol were present. Structure elucidation of **5** by means of NMR spectroscopy corroborated the presence of included water and methanol. However, the presence of tautomerism, internal salt formation, association, and protonation/deprotonation behaviour prohibited assignment of ^{1}H NMR signals to certain species of **5**. Interestingly enough these complications were also encountered for the precursor compounds **2** [16] and **3**, which displayed ^{1}H signal broadening of the benzimidazolyl proton signals due to dynamic effects of the exchangeable NH of the benzimidazole moiety. It was not possible to identify a single species of **5** by means of ^{1}H NMR temperature variation experiments in *DMSO* (55°C) and pyridine (80°C) because no sharpening of the pertinent signals at these elevated temperatures could be observed. It should be stressed, that the strong acidity of the *bay* phenolic proton observed in the titration experiment is in agreement with the hypericinoide and not an isohypericinoide constitution [20, 21] of **5**.

The heterocyclically appended hypericin derivative **5** was effective in the hypericin sensitized destruction of bilirubin, which has been established as a rapid means to assess sensitized production of singlet oxygen or reactive oxygen species [5]. However, it was necessary to slightly modify the conditions described in Ref. [22] because an interaction between **5** and bilirubinate was observed. This might occur from a salt formation between the propionic acid side chains of bilirubin IXα with the basic benzimidazolyl substituents of **5**. By adding benzimidazole to both test solutions as described in the experimental part it was possible to start from a defined stabilized starting point after a 1 h equilibration time. In contrast to previously

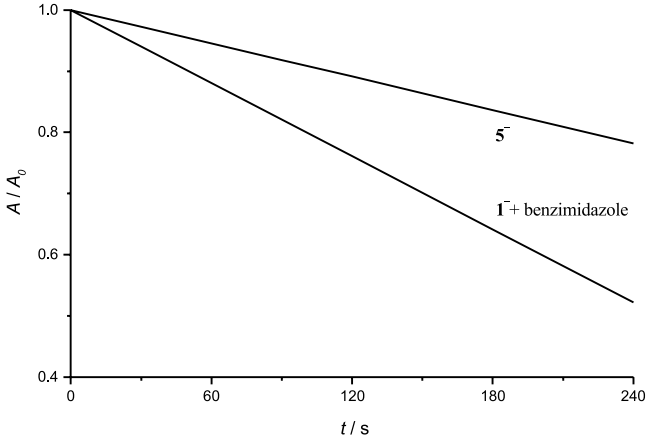

Fig. 2. Hypericin derivative sensitized photooxidation of bilirubin IXα: normalized absorption (A/A_0) *vs.* time curves of solutions of disodium bilirubinate IXα together with benzimidazole plus sodium hypericinate ($^{-3}$**1**) and the sodium salt of dibenzimidazolyl hypericin ($^{-3}$**5**) in aereated 80% aqueous *Et*OH with additional 5% *DMSO* as solution mediator upon irradiation at $\lambda > 570$ nm

described nitrogen containing hypericin derivatives [17], the heterocyclically appended hypericin derivative **5** showed the ability to sensitize singlet oxygen or corresponding reactive oxidative species. As can be derived from Fig. 2, hypericin (**1**), and to a somewhat lesser extent, the dibenzimidazolyl didesmethyl hypericin are quite effective singlet oxygen or reactive oxygen species sensitizers, which is *inter alia* important for the potential application of **5** in photodynamic therapy.

Semiempirical Calculations

To clarify the role of tautomerism of **5** it was investigated by means of semiempirical calculations (AM1). According to previous calculations by a variety of methods on hypericin (**1**) it is known that ten different tautomers are possible for **1**, were the $\mathbf{Q}^{7,14}$ tautomer ($\mathbf{Q}^{m,n}$ denotes the type of tautomer by indicating the carbonyl positions in superscripts) represents the most stable one [23–28]. For each tautomer of **1** two conformations, namely the ''propeller'' and ''butterfly'' conformation, might exist.

Calculations for the dibenzimidazolyl didesmethyl hypericin **5** were executed on the propeller conformation only because the butterfly conformers proved to be of higher energy in selected cases. In principle, there are two, three, or four carbonyl groups possible in the structure of **5**. Thus, there are ten different tautomers of the $\mathbf{Q}^{m,n}$-**5** type, with four possible conformations depending on the orientation of the benzimidazolyl substituents (*anti* or *syn*) for any of these species (Fig. 3). Tautomers with symmetric positions of their carbonyl groups have identical conformations of the *anti,syn*-type. Accordingly, overall there are 36 conformations of the type $\mathbf{Q}^{m,n}$ possible. For the $\mathbf{Q}^{m,n,o}$-**5** type 18 tautomers may exist in 36 conformations, whereas the three tautomers of $\mathbf{Q}^{m,n,o,p}$-**5** type display only one conformation each (Fig. 4).

As a summary, Fig. 5 presents the heats of formation of the conformations of **1** and **5** which are possible in principle. As observed for a variety of substituted

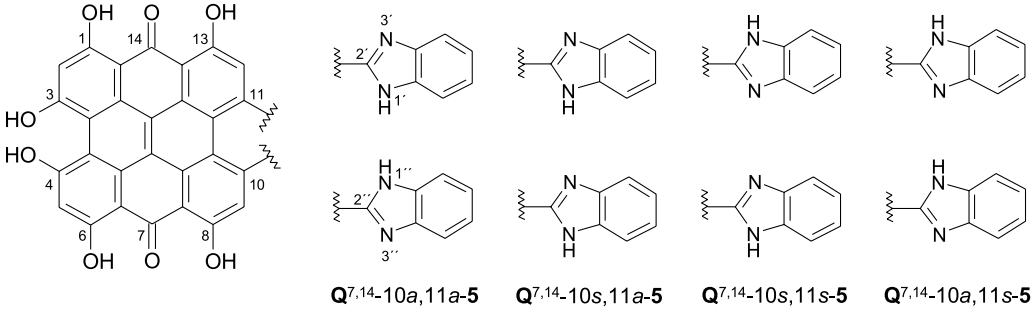

Fig. 3. Conformations of **5** depending on the orientation of the benzimidazolyl substituents (*a* .... *antiperiplanar – anticlinal*, *s* .... *synperiplanar – synclinal*)

hypericin derivatives [24–26] the 7,14-tautomer of **5** is by far ($\sim$50 kJ · mol^{-1}) the most stable one. This has been proven for **1** also by experimental means [23], which are, however, not directly applicable to the case of **5**. Tautomer $\mathbf{Q}^{7,14}$-10*a*,11*s*-**5** appears to be stabilized by 46.2 kJ · mol^{-1} compared to $\mathbf{Q}^{1,7}$-10*s*,11*s*-**5**. All other tautomeres are even less stable. Except for $\mathbf{Q}^{7,14}$-10*a*,11*s*-**5** and $\mathbf{Q}^{1,7}$-11*s*,11*s*-**5** the $\mathbf{Q}^{m,n}$-10*a*,11*a*-**5** conformation turned out to be the most stable one. In the case of the $\mathbf{Q}^{m,n,o}$ type tautomers there are no large gaps in the heats of formation. For $\mathbf{Q}^{1,4,8}$, $\mathbf{Q}^{3,4,8}$, $\mathbf{Q}^{1,4,13}$, and $\mathbf{Q}^{1,4,14}$ the 10*a* conformation is more stable than the 10*s*, for all other tautomers 10*s* is more stable. Comparison of the heats of formation of those tautomers showed that the most important influence on stability is the degree of aromaticity, which is optimal in case of the $\mathbf{Q}^{m,n}$ tautomers, especially $\mathbf{Q}^{7,14}$. As the number of quinoid rings increases the heat of formation increases concomitantly. So it seems unlikely that other tautomers than $\mathbf{Q}^{7,14}$-**5** are stable enough to be present in solutions of **5**. Accordingly, tautomerism seems to be not the reason for the problems discussed above concerning NMR spectroscopy. These problems obviously stem from the presence of protonation/deprotonation and association equilibria as well as conformational and proton exchange processes.

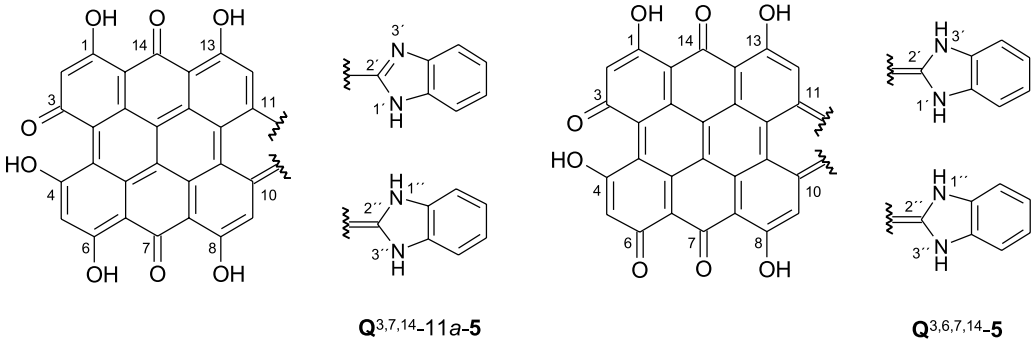

Fig. 4. Tautomers of type $\mathbf{Q}^{m,n,o}$ and $\mathbf{Q}^{m,n,o,p}$; benzimidazolyl substituents with two pyrrolic nitrogens are symmetrical and therefore no *antiperiplanar* to *anticlinal* or *synperiplanar* to *synclinal* conformations are possible

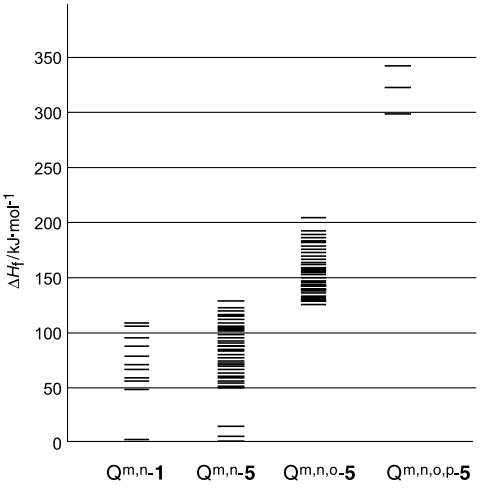

Fig. 5. The heat of formation differences of $\mathbf{Q}^{m,n}$-**1** are included as a reference [16] for the species of **5**; $\mathbf{Q}^{7,14}$-**1** is the standard for all other tautomers of **1**; for all conformations of **5**, $\mathbf{Q}^{7,14}$-**5** is the standard; the lowest three bars represent the conformations of $\mathbf{Q}^{7,14}$-**5**, which are $\mathbf{Q}^{7,14}$-10*a*,11*s*-**5**, $\mathbf{Q}^{7,14}$-10*s*,11*s*-**5**, $\mathbf{Q}^{7,14}$-10*a*,11*a*-**5** in descending order; the remaining bars represent all other conformations of **5**; the relative stability of tautomers in descending order is: **1**: $\mathbf{Q}^{7,14}$, $\mathbf{Q}^{1,7}$, $\mathbf{Q}^{3,7}$, $\mathbf{Q}^{7,13}$, $\mathbf{Q}^{1,6}$, $\mathbf{Q}^{1,4}$, $\mathbf{Q}^{8,13}$, $\mathbf{Q}^{1,8}$, $\mathbf{Q}^{3,4}$, $\mathbf{Q}^{3,8}$; **5**-$\mathbf{Q}^{m,n}$: $\mathbf{Q}^{7,14}$, $\mathbf{Q}^{7,13}$, $\mathbf{Q}^{1,7}$, $\mathbf{Q}^{3,7}$, $\mathbf{Q}^{8,13}$, $\mathbf{Q}^{1,6}$, $\mathbf{Q}^{1,4}$, $\mathbf{Q}^{1,8}$, $\mathbf{Q}^{3,4}$, $\mathbf{Q}^{3,8}$; **5**-$\mathbf{Q}^{m,n,o}$: $\mathbf{Q}^{1,4,8}$, $\mathbf{Q}^{7,8,14}$, $\mathbf{Q}^{3,7,14}$, $\mathbf{Q}^{4,7,14}$, $\mathbf{Q}^{1,7,13}$, $\mathbf{Q}^{1,6,8}$, $\mathbf{Q}^{1,6,13}$, $\mathbf{Q}^{1,4,7}$, $\mathbf{Q}^{1,7,8}$, $\mathbf{Q}^{3,4,8}$, $\mathbf{Q}^{1,4,13}$, $\mathbf{Q}^{1,7,14}$, $\mathbf{Q}^{3,7,8}$, $\mathbf{Q}^{6,7,14}$, $\mathbf{Q}^{3,4,7}$, $\mathbf{Q}^{1,6,7}$, $\mathbf{Q}^{1,6,14}$, $\mathbf{Q}^{1,4,14}$; **5**-$\mathbf{Q}^{m,n,o,p}$: $\mathbf{Q}^{3,4,7,14}$, $\mathbf{Q}^{1,4,7,14}$, $\mathbf{Q}^{1,6,7,14}$

In conclusion, the novel heterocyclically appended hypericin derivative **5** displays a pronounced bathochromic shift as compared to the parent system **1**. The potential of **5** for its application for photodynamic therapy is provided by this shift together with its ability to sensitize singlet oxygen or reactive oxygen species upon irradiation. The highly complicated structural system given by the benzimidazolyl moieties leading to a decreased extinction coefficient of the long wavelength band and its rather limited solubility in aqueous solvents are drawbacks, which should be possible to overcome. Nevertheless, **5** presents an important and valuable lead structure upon which future developments should be possible. Such investigations are presently underway in our laboratory.

Experimental

Solvents were of *p.a.* quality. *DMF* was freshly distilled prior to use. Melting points were measured on a *Kofler* melting point microscope (*Reichert*; Vienna). ^{1}H NMR were recorded on a Bruker Avance DRX 500 MHz spectrometer using a TXI cryoprobe with *z*-gradient coil. Standard temperature for NMR experiments in *DMSO* was 30°C. ^{1}H NMR temperature variation experiments of **5** were performed in *DMSO* and pyridine up to 55 and 80°C. 2D NMR experiments were performed on the 500 MHz spectrometer using standard pulse sequences as provided by the manufacturer. Typical 90° hard pulse durations were 8.2 µs (^{1}H) and 16.6 µs (^{13}C), 90° pulses in decoupling experiments were set to 67 µs. HSQC and HMBC experiments were optimized for coupling constants of 145 Hz for single quantum correlations and 10 Hz for multi-bond correlations. N*O*ESY mixing time was set to 400 ms. IR, UV/Vis, fluorescence, and mass spectra were recorded using the Bruker Tensor 27, Varian Cary 100 Bio UV/Vis, Hitachi 4010F, and Hewlett Packard 59987 quadrupole instrument. Elemental

analysis was performed at the microanalytical laboratory (Department of Physical Chemistry of the University of Vienna). Hypericin sensitized photooxidation of bilirubinate IXα was executed in slight modification according to Ref. [22]. Thus, the molar ratio of bilirubinate IXα:**5** was 2:1 and the mixture was flushed with Ar and kept in the dark for 1 h before starting the hypericin sensitized photooxidation. This procedure was necessary because of the interaction of the basic benzimidazolyl NH protons with the carboxylate groups of the bilirubinate IXα. Therefore the reference experiment was performed with a mixture of bilirubinate IXα:benzimidazole:**1** in a molar ratio of 2:2:1. Because of the poor solubility of **5** in 80% aqueous *Et*OH all solutions were prepared by using 5% *DMSO* as a solution mediator. Spectrophotometric titration of **5** was carried out in 80% aqueous *DMSO* using H_2SO_4 or tetrabutylammonium hydroxide (*TBAH*) as acid or base [20]. For mass spectroscopic [21] and fluorescence experiments the *pH* values were adjusted by means of buffered aqueous solutions (*e.g.* $HCOO^-NH_4^+$/HCOOH, KCl/HCl, Na_2CO_3/NaOH, as well as HCl and NaOH) instead of distilled H_2O. Compound **2** (prepared according to Ref. [16]) was judged to be pure (>97%) by means of its ^{1}H NMR spectra and chromatography. Semiempirical calculations were performed at the SGI Origin 3800 of the ZID at the Johannes Kepler University of Linz with AM1 [29] using inputs from MM3 [30].

6-(1H-Benzimidazol-2-yl)-1,3,8-trihydroxy-10H-anthracen-9-one (**3**, $C_{21}H_{14}N_2O_4$)

To a refluxing solution of 83.3 mg of **2** (0.201 mmol) in 17 cm^3 of glacial acetic acid under Ar, 362.8 mg of $SnCl_2 \cdot 2H_2O$ (1.608 mmol) in 7.5 cm^3 of HBr (47% aq) were added. The resulting mixture was refluxed for 1 h, cooled, poured onto ice/H_2O, and centrifuged. The residue was washed three times with distilled H_2O and dried over night in vacuum over P_4O_{10} to yield 68.0 mg (94%) of **3**. Mp 239–240°C (decomp.); TLC: $R_f = 0.92$ ($CHCl_3$:CH_3OH = 2:1), $R_f = 0.00$ ($CHCl_3$:$CH_3COOC_2H_5$ = 3:1); ^{1}H NMR (500 MHz, *DMSO*-d_6): $\delta = 13.49$ (br. s, NH), 12.43 (s, 8-OH), 12.33 (s, 1-OH), 10.95 (s, 3-OH), 7.81 (d, $J = 1.1$ Hz, ar-H5), 7.65–7.64 (m, 2ar-H), 7.63 (d, $J = 1.1$ Hz, ar-H7), 7.29–7.26 (m, 2ar-H), 6.50 (d, $J = 2.2$ Hz, ar-H4), 6.27 (d, $J = 2.2$ Hz, ar-H2), 4.49 (s, 10-CH_2) ppm; N*O*ESY (*DMSO*-d_6): 1-O*H* ↔ ar-*H*2, 3-O*H* ↔ ar-*H*2 and ar-*H*4, 8-O*H* ↔ ar-*H*7, 10-C*H*$_2$ ↔ ar-*H*4 and ar-*H*5, ar-*H*4′/ar-*H*7′ ↔ ar-*H*5′/ar-*H*6′; ^{13}C NMR (125 MHz, *DMSO*-d_6): $\delta = 190.7$ (C9), 165.4 (C3), 164.7 (C1), 161.9 (C8), 149.4 (br., C=N), 145.1 (C4a), 142.9 (C10a), 135.2 (br., C6), 123.2–123.0 br. (C4′, C5′, C6′, and C7′), 116.9 (C5), 115.9 (C8a), 115.3 (br., C3a′ and C7a′), 112.2 (C7), 108.6 (C9a), 107.6 (C4), 101.1 (C2), 32.53 (C10) ppm; HSQC (*DMSO*-d_6): ar-*H*2 ↔ *C*2, ar-*H*4 ↔ *C*4, ar-*H*5 ↔ *C*5, ar-*H*7 ↔ *C*7, 10-C*H*$_2$ ↔ 10-*C*H$_2$, ar-*H*4′/ar-*H*5′ ↔ *C*4′/*C*5′, ar-*H*5′/ar-*H*6′ ↔ *C*5′/*C*6′; HMBC (*DMSO*-d_6): *C*1 → 1-O*H* and ar-*H*2, *C*2 → 1-O*H*, 3-O*H* and ar-*H*4, *C*3 → 3-O*H*, ar-*H*2 and ar-*H*4, *C*4 → ar-*H*2, 3-O*H* and 10-C*H*$_2$, *C*5 → ar-*H*7 and 10-C*H*$_2$, *C*6 → 8-O*H* and 10-C*H*$_2$, *C*7 → ar-*H*5 and 8-O*H*, *C*8 → 8-O*H* and ar-*H*7, *C*10 → ar-*H*4 and ar-*H*5, *C*4a → ar-*H*2, ar-*H*4, ar-*H*5 and 10-C*H*$_2$, *C*8a → ar-*H*5, ar-*H*7, 8-O*H* and 10-C*H*$_2$, *C*9a → ar-*H*2, ar-*H*4, 1-O*H* and 10-C*H*$_2$, *C*10a → ar-*H*5 and 10-C*H*$_2$, 2′-*C*=N → ar-*H*5 and ar-*H*7 – it noteworthy that the ^{13}C signals of C6, C3a′, C4′, C5′, C6′, C7′, and C7a′ are weak due to dynamic effects of the benzimidazolyl substituent; ESI-MS (*Me*OH + 1% NH_3, $\gamma = 1.0\,mg \cdot cm^{-3}$, negative ion mode): $m/z = 357$ ([M-H]$^-$); IR (KBr): $\bar{\nu} = 3474$ (br., OH, NH), 3053 (=CH), 2930, 2862 (CH-aliph), 1622 (CO), 1602 (C=N), 1480, 1381, 1340, 1277, 1248, 1171, 1159, 1060, 956, 845, 744 cm^{-1}; UV-Vis (*Me*OH): λ_{max}(rel. int.) = 211 (100), 317 (41), 376 (60) nm (%).

10,13-Bis-(1H-benzimidazol-2-yl)-1,3,4,6,8,15-hexahydroxydibenzo[ao]perylene-7,16-dione (**4**, $C_{42}H_{22}N_4O_8$)

A mixture of 73.2 mg of **3** (0.204 mmol), 2.84 mg of $FeSO_4 \cdot 7H_2O$ (0.010 mmol), and 103.9 mg of pyridine-*N*-oxide (1.093 mmol) in 1.1 cm^3 of absolute pyridine and 0.1 cm^3 of absolute piperidine was stirred under Ar with protection from light at 115°C for 1 h. After cooling down to room temperature the reaction mixture was poured into 8 cm^3 of 2 *M* HCl and stirred for 30 min at room temperature in

the dark. After centrifugation the residue was washed three times with 3% HCl, three times with distilled H_2O, and dried over night in vacuum over P_4O_{10} resulting in 64.3 mg of a mixture of **4** and **5**; due to its light sensitivity **4** could be characterized only by its mass spectrum: ESI-MS (*Me*OH + 1% NH_3, $\gamma = 1.0\,mg \cdot cm^{-3}$, negative ion mode): $m/z = 709$ ($[M\text{-}H]^-$ of **4**) and 707 ($[M\text{-}H]^-$ of **5**).

10,11-Bis-(1H-benzimidazol-2-yl)-1,3,4,6,8,13-hexahydroxyphenanthro[1,10,9,8-opqra]perylene-7,14-dione (**5**, $C_{42}H_{20}N_4O_8$)

A solution of 58.4 mg of a mixture of **4** and **5** (see above) in 1500 cm^3 of *Me*OH was irradiated for 35 min by means of a 700 W Hg high pressure lamp with fluorescence screen (Philips) under stirring and air admission. After evaporation of the solvent the resulting dark green solid was triturated with *Me*OH to yield 56.0 mg (85% based on **3**) of **5**. Mp >350°C; ESI-MS (*Me*OH, $\gamma = 1.0\,mg \cdot cm^{-3}$, negative ion mode): $m/z = 707$ ($[M\text{-}H]^-$); ESI-MS (*DMSO*:buffer = 4:1, $pH = 6.4$, $\gamma = 0.1\,mg \cdot cm^{-3}$, negative ion mode): $m/z = 707$ ($[M\text{-}H]^-$); ESI-MS (*DMSO*:buffer = 4:1, $pH = 10.0$, $\gamma = 0.1\,mg \cdot cm^{-3}$, negative ion mode): $m/z = 707$ ($[M\text{-}H]^-$); ESI-MS (*DMSO*:buffer = 4:1, $pH = 12.0$, $\gamma = 0.1\,mg \cdot cm^{-3}$, negative ion mode): $m/z = 707$ ($[M\text{-}H]^-$); IR (KBr): $\bar{\nu} = 3416$ (br., OH, NH), 2943, 2840 (CH-aliph), 1667 (CO), 1659 (CO), 1598 (C=N), 1566, 1486, 1460, 1427, 1375, 1350, 1325, 1254, 1222, 1203, 1167, 1133, 1070, 1054, 982, 946, 915, 886, 852, 812, 757, 657 cm^{-1}; UV-Vis (*DMF*, $c = 8.52 \cdot 10^{-6}\,mol \cdot dm^{-3}$): $\lambda_{max}(\varepsilon) = 306$ (33107), 571 (4576), 617 (8682), 671 (5279) nm ($dm^3 \cdot mol^{-1} \cdot cm^{-1}$); UV-Vis (*DMSO*, $c = 9.15 \cdot 10^{-6} mol \cdot dm^{-3}$): $\lambda_{max}(\varepsilon) = 311$ (28630), 396 (8851), 570 (5463), 617 (10928), 675 (4699) nm ($dm^3 \cdot mol^{-1} \cdot cm^{-1}$); UV-Vis (pyridine, $c = 7.73 \cdot 10^{-6} mol \cdot dm^{-3}$): $\lambda_{max}(\varepsilon) = 311$ (29119), 405 (8102), 573 (5435), 620 (10612), 679 (5565) nm ($dm^3 \cdot mol^{-1} \cdot cm^{-1}$); UV-Vis (*DMSO*:$H_2O$ = 4:1, $c = 9.96 \cdot 10^{-6}\,mol \cdot dm^{-3}$): $\lambda_{max}(\varepsilon) = 271$ (42256), 397 (9736), 570 (5320), 614 (9234), 669 (5220) nm ($dm^3 \cdot mol^{-1} \cdot cm^{-1}$); UV-Vis (*DMSO*:$H_2O$ = 4:1, $pH = 1.0$, $c = 9.96 \cdot 10^{-6}\,mol \cdot dm^{-3}$): $\lambda_{max}(\varepsilon) = 291$ (103835), 576 (4978), 618 (8732), 673 (5520) nm ($dm^3 \cdot mol^{-1} \cdot cm^{-1}$); UV-Vis (*DMSO*:$H_2O$ = 4:1, $pH = 3.0$, $c = 9.96 \cdot 10^{-6}\,mol \cdot dm^{-3}$): $\lambda_{max}(\varepsilon) = 307$ (22684), 501 (2007), 620 (6925) nm ($dm^3 \cdot mol^{-1} \cdot cm^{-1}$); UV-Vis (*DMSO*:$H_2O$ = 4:1, $pH = 6.4$, $c = 9.96 \cdot 10^{-6}\,mol \cdot dm^{-3}$): $\lambda_{max}(\varepsilon) = 307$ (26599), 571 (5220), 615 (9134), 673 (4919) nm ($dm^3 \cdot mol^{-1} \cdot cm^{-1}$); UV-Vis (*DMSO*:$H_2O$ = 4:1, $pH = 10.5$, $c = 9.96 \cdot 10^{-6}\,mol \cdot dm^{-3}$): $\lambda_{max}(\varepsilon) = 298$ (32285), 615 (10374), 653 (11020) nm ($dm^3 \cdot mol^{-1} \cdot cm^{-1}$); UV-Vis (acetone): λ_{max}(rel. int.) = 398 (100), 586 (80), 612 (95), 636 (77) nm (%); UV-Vis (acetonitrile): λ_{max}(rel. int.) = 355 (100), 569 (28), 612 (38), 642 (32) nm (%); UV-Vis (ethyl acetate): λ_{max}(rel. int.) = 569 (73), 613 (100), 671 (62) nm (%); UV-Vis (*Me*OH): λ_{max}(rel. int.) = 302 (100), 594 (17), 636 (21) nm (%); UV-Vis (*THF*): λ_{max}(rel. int.) = 308 (100), 396 (38), 569 (26), 616 (42), 649 (22) nm (%); dilution experiment: UV-Vis (*DMSO*:H_2O = 4:1, $d = 10\,mm$, $c = 2.34 \cdot 10^{-5}\,mol \cdot dm^{-3}$): $\lambda_{max}(\varepsilon) = 309$ (28760), 615 (9748) nm ($dm^3 \cdot mol^{-1} \cdot cm^{-1}$), UV-Vis (*DMSO*:$H_2O$ = 4:1, $d = 1\,mm$, $c = 2.34 \cdot 10^{-4}\,mol \cdot dm^{-3}$): $\lambda_{max}(\varepsilon) = 308$ (26181), 625 (7334) nm ($dm^3 \cdot mol^{-1} \cdot cm^{-1}$); fluorescence (*DMSO*, $c = 7.82 \cdot 10^{-7}\,mol \cdot dm^{-3}$, $\lambda_{ex} = 550\,nm$): λ_{em}(rel. int.) = 625 (99), 645 (100), 652 (95), 673 (84) nm (%); fluorescence (*DMSO*:buffer = 4:1, $pH = 0.1$, $c = 7.82 \cdot 10^{-7}\,mol \cdot dm^{-3}$, $\lambda_{ex} = 550\,nm$): λ_{em}(rel. int.) = 602 (29), 648 (98), 654 (100), 674 (91) nm (%); fluorescence (*DMSO*:buffer = 4:1, $pH = 1.0$, $c = 7.82 \cdot 10^{-7}\,mol \cdot dm^{-3}$, $\lambda_{ex} = 550\,nm$): λ_{em}(rel. int.) = 607 (27), 647 (98), 653 (100), 674 (90) nm (%); fluorescence (*DMSO*:buffer = 4:1, $pH = 2.1$, $c = 7.82 \cdot 10^{-7}\,mol \cdot dm^{-3}$, $\lambda_{ex} = 550\,nm$): λ_{em}(rel. int.) = 623 (92), 646 (100), 652 (95), 673 (85) nm (%); fluorescence (*DMSO*:buffer = 4:1, $pH = 3.1$, $c = 7.82 \cdot 10^{-7}\,mol \cdot dm^{-3}$, $\lambda_{ex} = 550\,nm$): λ_{em}(rel. int.) = 623 (74), 646 (100), 652 (98), 673 (88) nm (%); fluorescence (*DMSO*:buffer = 4:1, $pH = 5.0$, $c = 7.82 \cdot 10^{-7}\,mol \cdot dm^{-3}$, $\lambda_{ex} = 550\,nm$): λ_{em}(rel. int.) = 623 (73), 645 (100), 653 (98), 673 (87) nm (%); fluorescence (*DMSO*:buffer = 4:1, $pH = 6.4$, $c = 7.82 \cdot 10^{-7}\,mol \cdot dm^{-3}$, $\lambda_{ex} = 550\,nm$): λ_{em}(rel. int.) = 623 (79), 645 (100), 652 (97), 674 (86) nm (%); fluorescence (*DMSO*:buffer = 4:1, $pH = 10.0$, $c = 7.82 \cdot 10^{-7}\,mol \cdot dm^{-3}$, $\lambda_{ex} = 550\,nm$): λ_{em} (rel. int.) = 623 (100), 645 (82), 673 (67) nm (%); fluorescence (*DMSO*:buffer = 4:1, $pH = 12.0$, $c = 7.82 \cdot 10^{-7}\,mol \cdot dm^{-3}$, $\lambda_{ex} = 550\,nm$): λ_{em}(rel. int.) = 594 (61), 608 (48), 647 (95), 655 (100), 673 (99) nm (%); fluorescence (*DMSO*:buffer = 4:1, $pH = 14.0$, $c = 7.82 \cdot 10^{-7}\,mol \cdot dm^{-3}$, $\lambda_{ex} = 550\,nm$):

λ_{em}(rel. int.) = 646 (96), 653 (100), 674 (93) nm (%); fluorescence (*DMF*, $c = 1.03 \cdot 10^{-6}$ mol · dm^{-3}, $\lambda_{ex} = 550$ nm): λ_{em}(rel. int.) = 625 (100), 676 (26) nm (%); fluorescence (pyridine, $c = 9.30 \cdot 10^{-7}$ mol · dm^{-3}, $\lambda_{ex} = 550$ nm): λ_{em}(rel. int.) = 627 (100), 677 (27) nm (%); elemental analysis: C 51.19%, H 4.79%, N 4.81% – this C, H, and N content of **5** is in good agreement with the calculated values (C 71.19%, H 2.84%, N 7.91%) considering the presence of tightly bound 21% methanol and 7% H_2O, which are also evident from the ^{1}H NMR spectra. It should be mentioned that excessive vacuum drying did not result in an improvement of the stated purity. The ε-values given in Fig. 1 were corrected for these crystal solvents.

Acknowledgements

The cryogenic 500 MHz NMR probe used was purchased from project P15380 (project leader: Norbert Müller) by FWF (Austrian Science Fund). Recording of ESI-MS by Prof. Dr. *C. Klampfl* and the generous allocation of cpu time by the ZID at the University of Linz is gratefully acknowledged.

References

[1] Falk H (1999) Angew Chem **111**: 3306; Angew Chem Int Ed **38**: 3116
[2] Obermüller RA, Hohenthanner K, Falk H (2001) Photochem Photobiol **74**: 211
[3] Obermüller RA, Etzlstorfer C, Falk H (2002) Monatsh Chem **133**: 89
[4] Lackner B, Falk H (2002) Monatsh Chem **133**: 717
[5] Thomas C, Pardini RS (1992) Photochem Photobiol **55**: 831
[6] Lavie G, Valentine F, Levin B, Mazur Y, Gallo G, Lavie D, Weiner D, Meruelo D (1989) Proc Natl Acad Sci USA **86**: 5963
[7] Agostinis P, Vantieghem A, Merlevede W, De Witte PAM (2002) Int J Biochem & Cell Biol **34**: 221
[8] Tran HTN, Falk H (2002) Monatsh Chem **133**: 1231
[9] Obermüller RA, Falk H (2001) Monatsh Chem **132**: 1519
[10] Dax TG, Falk H (2000) Monatsh Chem **131**: 1217
[11] Dax TG, Kapinus EI, Falk H (2000) Helv Chim Acta **83**: 1744
[12] Amer AM, Falk H, Tran HTN (1998) Monatsh Chem **129**: 1237
[13] Falk H, Sarhan AAO, Tran HTN, Altmann R (1998) Monatsh Chem **129**: 309
[14] Altmann R, Falk H, Gruber HJ (1998) Monatsh Chem **129**: 235
[15] Salama TA, Lackner B, Falk H (2003) Monatsh Chem **134**: 1113
[16] Salama TA, Lackner B, Falk H (2004) Monatsh Chem **135** (in press)
[17] Obermüller RA, Falk H (2001) Monatsh Chem **132**: 1519
[18] Falk H, Meyer J, Oberreiter M (1993) Monatsh Chem **124**: 339
[19] Grimmett MR (1984) Comprehensive Heterocyclic Chemistry Vol 5 Part 4A Potts KT (ed) Pergamon Press
[20] Altmann R, Falk H (1997) Monatsh Chem **128**: 571
[21] Ahrer W, Falk H, Tran HTN (1998) Monatsh Chem **129**: 643
[22] Hagenbuchner K, Falk H (1999) Monatsh Chem **130**: 1075
[23] Etzlstorfer C, Falk H, Müller N, Schmitzberger W, Wagner UG (1993) Monatsh Chem **124**: 751
[24] Etzlstorfer C, Falk H (1993) Monatsh Chem **124**: 1031
[25] Etzlstorfer C, Falk H (1994) Monatsh Chem **125**: 955
[26] Etzlstorfer C, Falk H, Müller N (1993) Monatsh Chem **124**: 431
[27] Gutman I (1999) Theochem **460**: 47
[28] Gutman I, Marković Z, Solujić S, Sukdolak S (1998) Monatsh Chem **129**: 481
[29] MOPAC 6.0 DEC-3100 Ed 1990, FJ Seiler Res Lab, USAF Acad80840
[30] Tinker 4.0, Ponder JW 2003, http://dasher.wustl.edu/tinker